

Certified Reduced Order Methods for Optimal Treatment Planning

Bahodir Ahmedov, Martin A. Grepl and Michael Herty

Institut für
Geometrie und Praktische Mathematik
Templergraben 55, 52062 Aachen, Germany

Bahodir Ahmedov, Aachen Institute for Advanced Study in Computational Engineering Science (AICES),
RWTH Aachen University, Schinkelstr. 2, 52062 Aachen, Germany, ahmedov@ices.rwth-aachen.de
Martin A. Grepl, Institut für Geometrie und Praktische Mathematik, RWTH Aachen University,
Templergraben 55, 52056 Aachen, Germany, grepl@igpm.rwth-aachen.de
Michael Herty, Institut für Geometrie und Praktische Mathematik, RWTH Aachen University,
Templergraben 55, 52056 Aachen, Germany, herty@igpm.rwth-aachen.de

Mathematical Models and Methods in Applied Sciences
 © World Scientific Publishing Company

Certified Reduced Order Methods for Optimal Treatment Planning

Bahodir Ahmedov

*Aachen Institute for Advanced Study in Computational Engineering Science (AICES),
 RWTH Aachen University,
 Schinkelstr. 2, 52062 Aachen, Germany
 ahmedov@aices.rwth-aachen.de*

Martin A. Grepl

*Institut für Geometrie und Praktische Mathematik, RWTH Aachen University,
 Templergraben 55, 52056 Aachen, Germany,
 grepl@igpm.rwth-aachen.de*

Michael Herty

*Institut für Geometrie und Praktische Mathematik, RWTH Aachen University,
 Templergraben 55, 52056 Aachen, Germany,
 herty@igpm.rwth-aachen.de*

Received (Day Month Year)

Revised (Day Month Year)

Communicated by (xxxxxxxxxx)

We study numerical methods for inverse problems arising in cancer therapy treatment under uncertainty. The interest is on efficient and reliable numerical methods that allow to determine the influence of possible unknown parameters on the treatment plan for cancer therapy. The Boltzmann transport equation is used to model the evolution of charged particles in tissue. A mixed variational framework is presented and existence and uniqueness of a weak solution is established. The optimality system is approximated using a low-dimensional reduced basis formulation based on a P_N -FE discretization. We derive *a posteriori* bounds for the error in the reduced basis solution of the optimal control problem with respect to the solution of the P_N -FE discretization. Numerical results in slab geometry are presented to confirm the validity of our approach.

Keywords: optimal radiotherapy, reduced basis methods, *a posteriori* error estimation, P_N - methods, mixed variational formulation

AMS Subject Classification: 85A25, 49J20, 65K10, 65M15, 92C50

1. Introduction

We are interested in the numerical discretization of inverse problems in cancer therapy. In particular, we focus on treatment planning using ionizing radiation. Several journal issues have been devoted to the topic of modeling and numerical analysis of cancer therapy and we refer to Refs. 6, 7, 8, 9 for more details. Here, we focus on

radiation treatment of patients. The aim of radiation treatment is to deposit enough energy in cancer cells so that they are destroyed while healthy tissue around the cancer cells should be harmed as little as possible.

The design of the precise treatment plan and the corresponding dose computation based on the geometry of the cancer as well as healthy cells is still a topic of active research. We follow here an approach requiring mathematical modeling and optimization techniques³⁶; for a review on existing technologies we refer to Refs. 11, 21. The mathematical modeling of dose calculation using a Boltzmann transport has recently gained attention^{23,29,37,39,19,24}. It has been argued that the Boltzmann transport based dose calculations have the same computational complexity and accuracy as Monte Carlo simulations¹⁰. However, as opposed to the Monte Carlo methods, they allow to exploit structural information for analytical and numerical purposes^{38,19}. For optimal treatment planning problems governed by the Boltzmann transport equation a variety of analytical and numerical results could therefore be established over the past years.

The focus of the present paper is on the numerical analysis of dose computation problems. In particular, we investigate the dependence of the optimal treatment plan with respect to uncertain parameters of the problem. The guiding example is the location of tissue cells with different radiative properties. In practice, those are obtained through imaging processes and may only be reliable up to a certain error. A quantification of the effect of this error on the optimal treatment plan and a fast recomputation of the dose for online adjustment of treatment plans is certainly desirable. A first attempt using feedback control has been studied in Ref. 17.

Here, we proceed differently and pursue the reduced basis (RB) method, a model order reduction technique which allows for a low-dimensional approximation of the parametrized problem. Various model order reduction techniques have been employed over the past years to speed up the solution of optimal control problems, e.g., proper orthogonal decomposition (POD)⁴⁰, reduction based on inertial manifolds²⁵, and RB methods^{22,32,27}. However, since the solution of the reduced optimal control problem is generally suboptimal, rigorous and efficiently evaluable *a posteriori* error bounds are crucial to assess the quality of the solution^{22,28,32,40}. To this end, we first introduce a variational formulation of the Boltzmann transport equation — previously studied in the context of forward simulation in Refs. 14, 15, 16 — and extend the discretization towards the treatment planning problem. We also note that an RB approach for a Boltzmann model has been previously considered in Ref. 33 and transport-dominated problems in Ref. 12. Based on the work in Ref. 28, we then develop efficient and reliable *a posteriori* error bounds for the reduced basis solution to the radiation treatment planning problem, i.e., for the error in the optimal control and the associated cost functional. Finally, we employ the reduced solution to quantify L^∞ and L^2 -deviations of the treatment plan in terms of the uncertainty in the geometry parameters.

In the following we present more details on the optimal treatment planning problem. The starting point is the Boltzmann equation for particle transport in

a medium: consider a part of the patient's body which contains the region of the cancer cells. We will consider the special case of a one-dimensional slab geometry. In slab geometry, the Boltzmann equation for particle transport reads

$$\mu \partial_x \psi(x, \mu) + \sigma_t(x) \psi(x, \mu) = \sigma_s(x) \int_{-1}^1 s(x, \mu \cdot \mu') \psi(x, \mu') d\mu' + q(x). \quad (1.1)$$

Here, ψ can be thought of as being the number of particles at $x \in [0, 1]$ and $\mu \in [-1, 1]$. The direction μ is the cosine of the angle between the direction and the x -axis. Scattering is determined by the total cross-section σ_t and by the total scattering cross-section σ_s . It is clear that the values of $\sigma_{t,s}$ *strongly dependent* on the underlying geometry: Scattering and adsorption is by magnitudes different in water and bone tissue. The geometry of the patient will therefore be encoded into those functions. The function $q(x)$ is the treatment plan (or control) and acts as an external source independent of μ . The function $s : \mathbb{R}^2 \rightarrow \mathbb{R}$ is the scattering kernel and given in case of radiotherapy for example by the simplified Henvey-Greenstein kernel

$$s(x, \eta) := \frac{1 - g(x)^2}{4\pi(1 + g(x)^2 - 2g(x)\eta)^{3/2}},$$

where g is the average cosine of the scattering angle. For high energy particles, small angle and energy changes are very likely, thus the scattering kernel is very forward-peaked. Boundary conditions for (1.1) are prescribed at the inflow part, i.e., for $\mu > 0$ at $x = 0$ and for $\mu < 0$ at $x = 1$. At those points we prescribe zero boundary conditions $\psi(x, \mu) = 0$ for simplicity. Note that Equ. (1.1) is also the basic model for transport of non-interacting particles in astrophysics, neutron transport and other applications. It is referred to as the monochromatic radiative transfer equation^{13,26,18,15}.

As in Ref. 36, we assume that the amount of destroyed cells in a small volume, be they cancer or healthy cells, is directly proportional to the dose

$$D(x) = \int_{-1}^1 \psi(x, \mu) d\mu \quad (1.2)$$

deposited in that volume. The computational domain is divided into tumor tissue, normal tissue and a region at risk: $\Omega = [0, 1] = \Omega_T \cup \Omega_N \cup \Omega_R$. We prescribe a desired dose distribution $\bar{D}(x)$, which usually has a constant value in Ω_T and is zero elsewhere. The problem of optimal treatment planning is then to find an external beam distribution q such that

$$\bar{J}(\psi) = \frac{\alpha_T}{2} \int_{\Omega_T} (D - \bar{D})^2 dx + \frac{\alpha_N}{2} \int_{\Omega_N} (D - \bar{D})^2 dx + \frac{\alpha_R}{2} \int_{\Omega_R} (D - \bar{D})^2 dx$$

is minimal. Here, α_T , α_N , and α_R are (positive) weights determining the trade-off between the terms in the cost. Defining $\alpha(x) = \alpha_T \chi_T(x) + \alpha_N \chi_N(x) + \alpha_R \chi_R(x)$, where $\chi_{T,N,R}(x)$ are appropriate characteristic functions, we formulate the optimal

treatment planning problem therefore as

$$\min J(\psi, q) = \int_0^1 \frac{\alpha(x)}{2} (D - \bar{D})^2 dx + \frac{1}{2} \int_0^1 q(x)^2 dx \text{ subject to (1.1)}. \quad (1.3)$$

We are interested in the optimal treatment plan $q(x)$ obtained as the numerical solution to problem (1.3). Since material properties σ_t and σ_s may differ in various regions of the domain, we investigate the dependence of the optimal plan $q(x)$ on the geometry parameters. Often, during treatment geometry of materials may change. Since, re-planning (finding optimal plan $q(x)$ for new values of material parameters) is often expensive in terms of computational time, we apply the reduced basis method to the optimal control problem (1.3) which allows to efficiently investigate this parametric dependence.

The outline of the paper is as follows. In Section 2 we present a variational discretization similar to the one proposed in Ref. 14 and establish existence and uniqueness of the optimal control. In Section 3 we introduce the parametrized geometry as well as the parametrized optimal control problem. We state the first order optimality conditions and subsequently derive the P_1 -FEM numerical scheme for the solution of the radiative transfer equation (1.1). The reduced basis method for the parametrized optimal radiotherapy model is presented in Section 4, where we briefly explain the construction of the RB spaces. In Section 5 we develop *a posteriori* error bounds for the optimal control and the associated cost functional value. The performance of the *a posteriori* error bounds is shown in Section 6. Here, we also present numerical examples where we explore uncertainty properties of the optimal control when input parameters are subject to random variations. We try to meet the standards of reproducible research in the computation sciences, laid out e.g. by LeVeque³⁰. The source code, which is designed in MATLAB, along with files to generate all figures and results of the paper, as well as additional functions and examples, are available online¹.

2. Mixed Variational Formulation

2.1. Boltzmann Equation

We introduce a variational formulation of Eq. (1.1) and problem (1.3) in order to apply reduced order modeling techniques. The variational formulation of (1.1) has been studied among others in Ref. 15 and we follow here closely their presentation. We denote by $\mathcal{D} := [0, 1] \times [-1, 1]$ the bounded convex domain of the problem and also define the spatial domain $\mathcal{I} := [0, 1]$. We next introduce the L^2 -scalar products $(\cdot, \cdot)_{\mathcal{D}}$ and $(\cdot, \cdot)_{\mathcal{I}}$ and induced norms $\|\cdot\|_{\mathcal{D}}^2 = (\cdot, \cdot)_{\mathcal{D}}$ and $\|\cdot\|_{\mathcal{I}}^2 = (\cdot, \cdot)_{\mathcal{I}}$ on the sets \mathcal{D} and \mathcal{I} , respectively. The inflow boundary is denoted by $\mathcal{D}_+ := \{(x, \mu) : x = 0, \mu > 0 \text{ or } x = 1, \mu < 0\}$, the remaining boundary by $\mathcal{D}_- = \partial\mathcal{D} \setminus \mathcal{D}_+$. In view of the arising operators we define the Lebesgue space of square integrable functions over \mathcal{D} and \mathcal{I} as $X := L^2(\mathcal{D})$ and $Y := L^2(\mathcal{I})$ with scalar products $(\psi, \phi)_X = (\psi, \phi)_{\mathcal{D}}$ and $(\psi, \phi)_Y = (\psi, \phi)_{\mathcal{I}}$; furthermore, we introduce $\mathbb{X} := \{\psi \in X : \mu \partial_x \psi \in X\}$ and

$\mathbb{X}_{bc} := \{\psi \in \mathbb{X} : \psi = 0 \text{ on } \mathcal{D}_+\}$.

Following Refs. 13, 19, we impose the following assumptions on the coefficients in Eq. (1.1)

$$s, \sigma_t, \sigma_s \geq 0, \quad \sigma_t(x), \sigma_s(x) \in L^\infty(\mathcal{I}), \quad \int_{-1}^1 s(x, \eta) d\eta \leq c_0, \quad \forall x \in \mathcal{I}, \quad (2.1a)$$

$$\sigma_t(x) - \sigma_s(x) \int_{-1}^1 s(x, \eta) d\eta \geq \hat{\beta} > 0, \quad \forall x \in \mathcal{I}, \quad (2.1b)$$

and define the transport and source term operator as

$$\mathcal{A} : \mathbb{X} \rightarrow X, \quad \mathcal{A}\psi = \mu \partial_x \psi, \quad (2.2)$$

$$\mathcal{C} : X \rightarrow X, \quad \mathcal{C}\psi = \sigma_t \psi - \sigma_s \int s(x, \mu \cdot \mu') \psi(x, \mu') d\mu'. \quad (2.3)$$

We can then restate Eq. (1.1) as an operator equation on \mathbb{X} and a strong solution $\psi \in \mathbb{X}_{bc}$ fulfills

$$\mathcal{A}\psi + \mathcal{C}\psi = q, \quad a.e. (x, \mu) \in \mathcal{D}. \quad (2.4)$$

The main properties of the operators (2.2) and (2.3) have been analysed for example in Ref. 13 and are summarized as follows: Under assumption (2.1), \mathcal{A} is a linear and bounded operator, and \mathcal{C} is linear, self-adjoint with respect to X , bounded, coercive and therefore invertible. The estimations on \mathcal{C} are as follows:

$$\begin{aligned} (C\phi, \phi)_{\mathcal{D}} &\leq \|\sigma_t\|_{L^\infty} \|\phi\|_{\mathcal{D}}^2 + \|\sigma_s\|_{L^\infty} \left\| \int \sqrt{s(x, \mu\mu')} \phi(x, \mu') \sqrt{s(x, \mu'\mu)} \phi(x, \mu) dx d\mu d\mu' \right\| \\ &\leq (\|\sigma_t\|_{L^\infty} + 2\|\sigma_s\|_{L^\infty} c_0) \|\phi\|_{\mathcal{D}}^2, \\ (C\phi, \phi)_{\mathcal{D}} &\geq \int_{\mathcal{D}} \left(\sigma_t - \sigma_s \int_{-1}^1 s(x, \mu\mu') d\mu' \right) \phi^2(x, \mu) dx d\mu \geq \hat{\beta} \|\phi\|_{\mathcal{D}}^2. \end{aligned}$$

Furthermore, for any $q \in Y$, there exists a unique (strong) solution $\psi \in \mathbb{X}_{bc}$ to Eq. (1.1). Define the operator mapping q to ψ , i.e.,

$$\mathcal{E} : Y \rightarrow \mathbb{X}_{bc} \subset X, \quad \mathcal{E}(q) = \psi, \quad (2.5)$$

where ψ is the solution to (1.1). According to Ref. 19 the operator \mathcal{E} is a bounded linear operator on X and we have $\|\mathcal{E}(q)\|_X \leq \frac{1}{\hat{\beta}} \|q\|_Y$.

A variational formulation is obtained using an even-odd splitting in the velocity space given by

$$\psi^\pm(x, \mu) = \frac{1}{2} (\psi(x, \mu) \pm \psi(x, -\mu)).$$

The splitting suggests to search for solutions $\psi = \psi^+ + \psi^-$ having the regularity $\psi^+ \in \mathbb{X}$ and $\psi^- \in X$. The space of such functions is denoted by \mathcal{X} , i.e., $\mathcal{X} := \{\psi = \psi^+ + \psi^- : \psi^+ \in \mathbb{X}, \psi^- \in X\}$. We introduce the following scalar product

$$(v, w)_{\mathcal{X}} = (\mathcal{A}v^+, \mathcal{A}w^+)_{\mathcal{D}} + (v, w)_{\mathcal{D}} + (v^+, w^+)_{\mathcal{T}} \quad (2.6)$$

6 *B. Ahmedov, M.A. Grepl, M. Herty*

and associated norm $\|v\|_{\mathcal{X}}^2 = \|\mathcal{A}v^+\|_{\mathcal{D}}^2 + \|v\|_{\mathcal{D}}^2 + \|v^+\|_{\mathcal{T}}^2$ on \mathcal{X} , where

$$(v^+, w^+)_{\mathcal{T}} := \sum_{x \in \{0,1\}} \int_{-1}^1 |\mu| w^+(x, \mu) v^+(x, \mu) d\mu.$$

We derive the variational formulation of (1.1) for zero boundary conditions as follows. Assume $\psi \in \mathbb{X}$ is a strong solution. Multiplying (1.1) by a test function $\phi \in \mathbb{X}$ and integrating over \mathcal{D} yields

$$\begin{aligned} 0 &= \int_{\mathcal{D}} \mu (\psi_x^+ + \psi_x^-) (\phi^+ + \phi^-) dx d\mu \\ &\quad + \int_{\mathcal{D}} \left(\sigma_t \psi \phi - \sigma_s \int \psi(x, \mu') s(x, \mu' \cdot \mu) d\mu' \phi(x, \mu) \right) dx d\mu - \int_{\mathcal{D}} q \phi dx d\mu \\ &= \int_{\mathcal{D}} \mu (\phi^+ \psi_x^- + \phi^- \psi_x^+) dx d\mu + (C\phi, \psi)_{\mathcal{D}} - (q, \phi)_{\mathcal{D}}. \end{aligned}$$

At $x = 1$ we have $\psi^+(\mu) = \frac{1}{2}\psi(\mu) = \psi^-(\mu)$ for $\mu > 0$ and $\psi^+(\mu) = \frac{1}{2}\psi(-\mu) = -\psi^-(\mu)$ for $\mu < 0$ and vice versa at $x = 0$. Therefore, $\mu\psi^-(\mu) = |\mu|\psi^+(\mu)$ and $\mu\psi^-(\mu) = -|\mu|\psi^+(\mu)$. Hence, integration by parts yields

$$\int_{\mathcal{D}} \mu \phi^+ \psi_x^- dx d\mu = - \int_{\mathcal{D}} \mu \phi_x^+ \psi^- dx d\mu + \sum_{x \in \{0,1\}} \int_{-1}^1 |\mu| \phi^+(x, \mu) \psi^+(x, \mu) d\mu.$$

We thus define bilinear forms $b(\cdot, \cdot) : Y \times \mathcal{X} \rightarrow \mathbb{R}$ and $a(\cdot, \cdot) : \mathcal{X} \times \mathcal{X} \rightarrow \mathbb{R}$ by

$$b(q, \phi) = (q, \phi)_{\mathcal{D}} \tag{2.7}$$

$$a(\psi, \phi) = (\phi^-, \mathcal{A}\psi^+)_{\mathcal{D}} - (\psi^-, \mathcal{A}\phi^+)_{\mathcal{D}} + (C\phi, \psi)_{\mathcal{D}} + \tag{2.8}$$

$$\sum_{x \in \{0,1\}} \int_{-1}^1 |\mu| \phi^+(x, \mu) \psi^+(x, \mu) d\mu,$$

respectively; we refer to Ref. 15 for the case $\mathcal{D} = \mathbb{R}^2 \times \mathcal{S}^2$. Note that since C is self-adjoint, a is symmetric. Furthermore, b is bounded on \mathcal{X} since

$$b(q, \phi) \leq 2\|q\|_{\mathcal{I}}\|\phi\|_{\mathcal{D}} \leq 2\|q\|_{\mathcal{I}}\|\phi\|_{\mathcal{X}}.$$

Next, we prove that the bilinear form a is continuous and inf-sup stable. We first note that a is bounded since

$$\begin{aligned} a(\psi, \phi) &\leq \|\phi^-\|_{\mathcal{D}}\|\mathcal{A}\psi^+\|_{\mathcal{D}} + \|\psi^-\|_{\mathcal{D}}\|\mathcal{A}\phi^+\|_{\mathcal{D}} + \|C\phi\|_{\mathcal{D}}\|\psi\|_{\mathcal{D}} + \|\phi^+\|_{\mathcal{T}}\|\psi^+\|_{\mathcal{T}} \\ &\leq \gamma_a\|\phi\|_{\mathcal{X}}\|\psi\|_{\mathcal{X}}, \end{aligned}$$

where $\gamma_a = 4(\|\sigma_t\|_{L^\infty} + 2\|\sigma_s\|_{L^\infty c_0})$ and we used the Cauchy-Schwarz inequality and $\|\phi^-\|_{\mathcal{D}} \leq \|\phi\|_{\mathcal{D}}$. It remains to show the inf-sup stability which requires to prove the following two estimates

$$\sup_{\|w\|_{\mathcal{X}}=1} |a(v, w)| \geq \beta\|v\|_{\mathcal{X}} \quad \text{and} \quad \sup_{\|v\|_{\mathcal{X}}=1} |a(v, w)| \geq \beta\|w\|_{\mathcal{X}}.$$

Since a is symmetric it suffices to prove one of the above. In the case $w = 0$ there is nothing to prove. We obtain for $v \in \mathbb{X}$, $v \neq 0$ For $w = v$ and $w = \mathcal{A}v^+$ we obtain

$$a(v, v) = (Cv, v) + \|v^+\|_{\mathcal{T}}^2 \geq \hat{\beta}\|v\|_{\mathcal{D}}^2 + \|v^+\|_{\mathcal{T}}^2 \geq \min\{\hat{\beta}, 1\}(\|v\|_{\mathcal{D}}^2 + \|v^+\|_{\mathcal{T}}^2).$$

A simple computation shows that we have $(\mathcal{A}v^+)^+ = 0$, $(\mathcal{A}v^+)^- = \mathcal{A}v^+$, and therefore

$$\begin{aligned} a(v, \mathcal{A}v^+) &= ((\mathcal{A}v^+)^-, \mathcal{A}v^+)_{\mathcal{D}} - (v^-, \mathcal{A}(\mathcal{A}v^+)^+)_{\mathcal{D}} + (C\mathcal{A}v^+, v)_{\mathcal{D}} + ((\mathcal{A}v^+)^+, v^+)_{\mathcal{T}} = \\ &= \|\mathcal{A}v^+\|_{\mathcal{D}}^2 + (\mathcal{A}v^+, Cv)_{\mathcal{D}} \geq \|\mathcal{A}v^+\|_{\mathcal{D}}^2 - \|\mathcal{A}v^+\|_{\mathcal{D}}\|Cv\|_{\mathcal{D}} \geq \frac{1}{2}\|\mathcal{A}v^+\|_{\mathcal{D}}^2 - \frac{\gamma_a}{8}\|v\|_{\mathcal{D}}^2. \end{aligned}$$

Hence, for $w = v - \mathcal{A}v^+$ we obtain

$$a(v, w) \geq \min\left\{\frac{1}{2}, \min\{\hat{\beta}, 1\} - \frac{\gamma_a}{8}\right\} \|v\|_{\mathcal{X}}^2.$$

Since $\|w\|_{\mathcal{X}} \leq 2\|v\|_{\mathcal{X}}$ we obtain – provided that $\min\{\hat{\beta}, 1\} - \frac{\gamma_a}{8} > 0$ – the inequality

$$a(v, w) \geq \beta_{\text{LB}}\|v\|_{\mathcal{X}}\|w\|_{\mathcal{X}}$$

where

$$\beta_{\text{LB}} := \frac{1}{2} \min\left\{\frac{1}{2}, \min\{\hat{\beta}, 1\} - \frac{\gamma_a}{8}\right\}. \quad (2.9)$$

We summarize the findings as follows using the generalized Lax–Milgram Lemma, resp. Babuzka–Aziz Lemma^{3,4}.

Lemma 2.1. *Assume that the hypothesis (2.1) holds true. Assume further that*

$$\|\sigma_t\|_{L^\infty} + 2\|\sigma_s\|_{L^\infty}c_0 < 2\min\{\hat{\beta}, 1\}. \quad (2.10)$$

Then the bilinear form $a : \mathcal{X} \times \mathcal{X} \rightarrow \mathbb{R}$ defined in (2.8) is linear, bounded and inf-sup stable with respect to the norm on \mathcal{X} . Furthermore, the bilinear form $b(\cdot, \cdot) : Y \times \mathcal{X} \rightarrow \mathbb{R}$ is bounded on \mathcal{X} . The variational problem

$$a(\psi, \phi) = b(q, \phi), \quad \forall \phi \in \mathcal{X}, \quad (2.11)$$

thus has a unique solution $\psi \in \mathcal{X}$ which depends continuously on the data

$$\|\psi\|_{\mathcal{X}} \leq \frac{2}{\beta_{\text{LB}}}\|q\|_{\mathcal{I}}.$$

In the simplest case of constant s , σ_t and σ_s with s such that $c_0 = 1$ we have $\hat{\beta} = \sigma_t - \sigma_s =: \sigma_a$. We thus obtain the equivalent condition $\sigma_s < \frac{7}{3}\sigma_a$, indicating a ratio of absorption σ_a to scattering σ_s of roughly one-half.

8 *B. Ahmedov, M.A. Grepl, M. Herty*

2.2. Optimal Control Problem

From Lemma 2.1 we obtain the well-posedness of the control to state operator for the variational problem. We call this operator also \mathcal{E} and it is defined by

$$\mathcal{E} : Y \rightarrow \mathcal{X}, \quad \mathcal{E}(q) = \psi, \quad (2.12)$$

where ψ solves (2.11). According to the previous lemma \mathcal{E} is well-defined, \mathcal{E} is a linear and bounded operator since we have $\|\mathcal{E}(q)\|_{\mathcal{X}} \leq \frac{2}{\beta_{LB}} \|q\|_{\mathcal{I}}$. For notational convenience, we define the linear operator $\mathcal{L} : \mathcal{X} \rightarrow Y$ given by $\mathcal{L}\phi = \int_{-1}^1 \phi(x, \mu) d\mu$. The related optimization problem (1.3) using the variational formulation now reads

$$\min_{\psi \in \mathcal{X}, q \in Y} J(\psi, q) = \frac{1}{2} \int_{\mathcal{I}} \alpha(x) (\mathcal{L}\psi - \bar{D})^2 dx + \frac{1}{2} \int_{\mathcal{I}} q(x)^2 dx \quad (2.13)$$

$$\text{subject to } (\psi, q) \in \mathcal{X} \times Y \text{ solves } \mathcal{E}(q) = \psi. \quad (2.14)$$

It follows from our assumptions that there exists a unique optimal solution $(\psi^*, q^*) \in \mathcal{X} \times Y$ to (2.13)³¹; also see Ref. 19 for the specific case considered here. We summarize the result in the following proposition.

Proposition 2.1. *Assume that the hypothesis (2.1) and (2.10) hold true. Let $\bar{D} = \int \bar{\psi} d\mu$ with $\bar{\psi} \in X$ be given and assume $\alpha > 0$ with $\alpha \in L^\infty(\mathcal{I})$.*

The control problem (2.13) then admits a unique solution $q^ \in Y$. The functions $\psi^* \in \mathcal{X}$, $\lambda^* \in \mathcal{X}$, and $q^* \in Y$ are a local minimum provided that the following first-order optimality conditions are fulfilled*

$$a(\psi^*, \phi) = b(q^*, \phi), \quad \forall \phi \in \mathcal{X}, \quad (2.15)$$

$$a(\phi, \lambda^*) = (\alpha(\bar{D} - \mathcal{L}\psi^*), \mathcal{L}\phi)_Y, \quad \forall \phi \in \mathcal{X}, \quad (2.16)$$

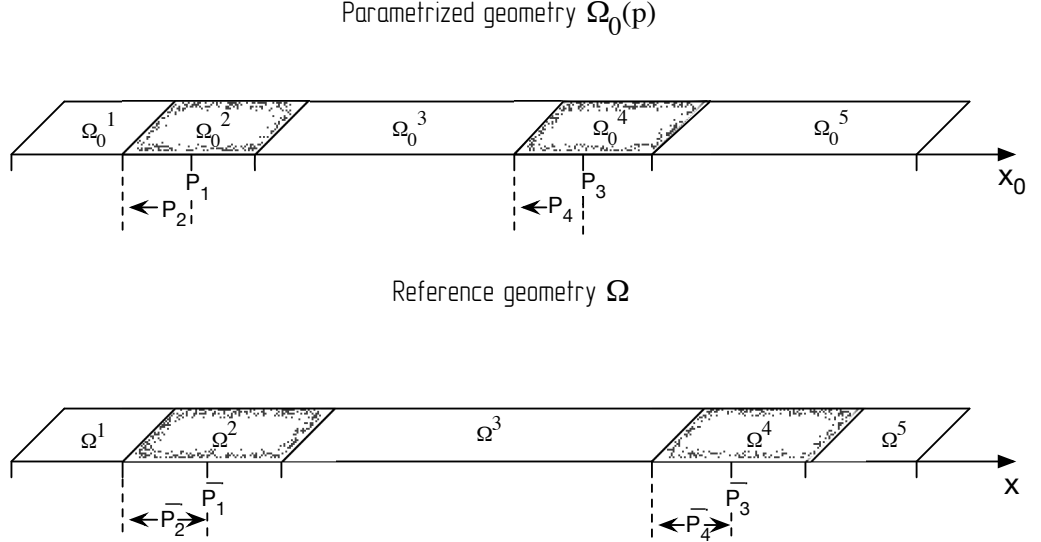
$$(q^*, \varphi)_Y - b(\varphi, \lambda^*) = 0, \quad \forall \varphi \in Y. \quad (2.17)$$

3. Parametrized Optimal Control Problem

3.1. Problem Statement

In radiotherapy treatment plan computations the spatial variation of the functions σ_t and σ_s depend on the geometry obtained from a CT scan of the patient's body. This geometry can only be determined up to a certain accuracy for reasons of movement of the patient during scanning. We are interested in a quantification of the optimal control q^* in terms of possible variations in σ_s and σ_t . We therefore consider a parametrized geometry and the associated parametrized optimal control problem. For simplicity we assume that the scattering kernel $s = s(x, \mu \cdot \mu')$ is independent of x . However, the approach presented can also be extended to x -dependent scattering kernels.

We consider the parametrized one-dimensional slab geometry sketched in Figure 1 on the top. We assume that the parametrized domain $\Omega_0(p)$ is divided into 5 subdomains $\Omega_0^i(p)$, $i = 1, \dots, 5$, which are described by four parameters

Fig. 1: Parametrized geometry $\Omega_0(p)$ and reference geometry Ω .

p_i , $i = 1, \dots, 4$: the parameters p_1 and p_2 (resp. p_3 and p_4) denote the center and half-width of the domain $\Omega_0^2(p)$ (resp. $\Omega_0^4(p)$). More precisely, we have $\Omega_0(p) = \cup_{i=1}^5 \Omega_0^i(p)$, where $\Omega_0^1(p) = \chi_{[0, p_1 - p_2]}(x)$, $\Omega_0^2(p) = \chi_{[p_1 - p_2, p_1 + p_2]}(x)$, $\Omega_0^3(p) = \chi_{[p_1 + p_2, p_3 - p_4]}(x)$, $\Omega_0^4(p) = \chi_{[p_3 - p_4, p_3 + p_4]}(x)$, and $\Omega_0^5(p) = \chi_{[p_3 + p_4, 1]}(x)$. We furthermore assume that the absorption and scattering coefficients σ_s and σ_t are known but possibly differ in the five subdomains so that we can write

$$\sigma_t(x) = \sum_{i=1}^5 \sigma_t^i \chi^i(x) \quad \text{and} \quad \sigma_s(x) = \sum_{i=1}^5 \sigma_s^i \chi^i(x), \quad (3.1)$$

where σ_t^i and σ_s^i , $i = 1, \dots, 5$, are given and the $\chi^i(x)$ are the characteristic functions corresponding to subdomain i . We denote the admissible parameter domain for our 4-tuple (input) geometry parameter by \mathcal{P} , i.e., $p = (p_1, p_2, p_3, p_4) \in \mathcal{P} \subset \mathbb{R}^4$.

The efficiency of the RB method relies on an offline-online computational decomposition which requires that all bilinear and linear forms satisfy an affine parameter dependence³⁴. To this end, we transform the parametrized geometry $\Omega_0(p)$ to a parameter-independent reference geometry Ω sketched in Figure 1 on the bottom. We then derive the weak formulation (2.11) for the reference geometry. The

10 *B. Ahmedov, M.A. Grepl, M. Herty*

parameter dependent forms can be written as

$$a(\psi, \phi; p) = \sum_{m=1}^{Q_a} \Theta_a^m(p) a^m(\psi, \phi), \quad \forall \psi, \phi \in \mathcal{X}, \quad (3.2)$$

$$b(q, \phi; p) = \sum_{m=1}^{Q_b} \Theta_b^m(p) b^m(q, \phi), \quad \forall q \in Y, \phi \in \mathcal{X}, \quad (3.3)$$

where the parameter-dependent coefficient functions $\Theta_{a,b}^m : \mathcal{P} \rightarrow \mathbb{R}$ are continuous and depend on p , but the bilinear forms $a^m(\cdot, \cdot) : \mathcal{X} \times \mathcal{X} \rightarrow \mathbb{R}$ and $b^m(\cdot, \cdot) : Y \times \mathcal{X} \rightarrow \mathbb{R}$ do *not* depend on p . We note that the bilinear form a satisfies the inf-sup condition

$$\beta(p) = \inf_{\psi \in \mathcal{X}} \sup_{\phi \in \mathcal{X}} \frac{a(\psi, \phi; p)}{\|\psi\|_{\mathcal{X}} \|\phi\|_{\mathcal{X}}} > 0, \quad (3.4)$$

where $\beta(p)$ is now parameter-dependent; similarly for the continuity of a and b . We summarize the expressions in Appendix A and refer to Ref. 2 for more details on the derivation.

We now state the parametrized optimal control problem as

$$\begin{aligned} \min_{\psi \in \mathcal{X}, q \in Y} J(\psi, q; p) &= \frac{1}{2} \int_{\mathcal{I}(p)} \alpha (\mathcal{L}\psi - \bar{D})^2 dx + \frac{1}{2} \int_{\mathcal{I}(p)} q(x)^2 dx \\ \text{s.t. } (\psi, q) &\in \mathcal{X} \times Y \text{ solves } a(\psi, \phi; p) = b(q, \phi; p), \quad \forall \phi \in \mathcal{X}. \end{aligned} \quad (3.5)$$

Note that the domain of integration, $\mathcal{I}(p)$, now also depends on the parameter p . It follows from Proposition 2.1 that there exists a unique optimal solution (ψ^*, q^*) to (3.5). Employing a Lagrangian approach, we again obtain the first-order optimality system consisting of the state equation, the adjoint equation, and the optimality equation: Given a parameter $p \in \mathcal{P}$, the optimal solution $(\psi^*, \lambda^*, q^*) \in \mathcal{X} \times \mathcal{X} \times Y$ satisfies

$$a(\psi^*, \phi; p) = b(q^*, \phi; p), \quad \forall \phi \in \mathcal{X}, \quad (3.6a)$$

$$a(\phi, \lambda^*; p) = (\alpha(\bar{D} - \mathcal{L}\psi^*), \mathcal{L}\phi)_{Y(p)}, \quad \forall \phi \in \mathcal{X}, \quad (3.6b)$$

$$(q^*, \varphi)_{Y(p)} - b(\varphi, \lambda^*; p) = 0, \quad \forall \varphi \in Y. \quad (3.6c)$$

3.2. P_N - Expansion

In general, we of course cannot expect to find an analytic solution to (3.6). We thus consider a tensor product approximation of (3.6): We employ a spectral P_N method for the angular domain and a finite element approach for the spatial domain. Since the state and the adjoint equations of the system (3.6) are structurally similar, we only present the numerical scheme for the state equation

$$a(\psi, \phi, p) = b(q, \phi; p), \quad \forall \phi \in \mathcal{X} \text{ and } q \in Y. \quad (3.7)$$

We express the angular dependence of the distribution function in terms of a Fourier series, i.e.,

$$\psi(x, \mu) = \sum_{\ell=0}^{\infty} \psi_{\ell}(x) \frac{2\ell+1}{2} P_{\ell}(\mu) \quad \text{and} \quad \phi(x, \mu) = \phi_k(x) P_k(\mu), \quad (3.8)$$

where P_{ℓ} are the Legendre polynomials of order ℓ and $\psi_{\ell}(x) \in Y$ for $\ell \in \mathbb{Z}$. Using properties of Legendre polynomials, we derive the even and odd components of ψ as

$$\psi^+ = \sum_{\ell} \psi_{2\ell}(x) \frac{4\ell+1}{2} P_{2\ell}(\mu) \quad \text{and} \quad \psi^- = \sum_{\ell} \psi_{2\ell+1}(x) \frac{4\ell+3}{2} P_{2\ell+1}(\mu) \quad (3.9)$$

By substituting the expansion into (3.7) we obtain (by suppressing the arguments and using properties of Legendre polynomials) the parameter dependent P_N equation

$$\sum_{m=1}^{Q_a} \Theta_a^m(p) a^m(\psi, \phi) = \sum_{m=1}^{Q_q} \Theta_q^m(p) b^m(q, \phi) \quad (3.10)$$

where $a^m(\psi, \phi)$ and $b^m(\psi, \phi)$ are defined as follows: for $m = 1, \dots, 6$

$$b^m(q, \phi) = \int_{\Omega^m} q_k(x) \phi_k(x) dx, \quad \text{for } k = 0, \dots,$$

for $m = 1, \dots, 5$

$$a^m(\psi, \phi) = \sigma_{tk}^m \int_{\Omega^m} \psi_k(x) \phi_k(x) dx,$$

for $m = 6$ and k odd

$$a^6(\psi, \phi) = \int_{\Omega} \phi_k(x) \left[\frac{k+1}{2k+1} \partial_x \psi_{k+1}(x) + \frac{k}{2k+1} \partial_x \psi_{k-1}(x) \right] dx,$$

for $m = 6$ and k even

$$\begin{aligned} a^6(\psi, \phi) = & - \int_{\Omega} \partial_x \phi_k(x) \left[\frac{k+1}{2k+1} \psi_{k+1}(x) + \frac{k}{2k+1} \psi_{k-1}(x) \right] dx + \\ & \sum_{\ell=0}^{\infty} \int_{-1}^1 |\mu| \phi_k(0) \psi_{\ell}(0) \frac{2\ell+1}{2} P_{\ell} P_k d\mu + \sum_{\ell=0}^{\infty} \int_{-1}^1 |\mu| \phi_k(1) \psi_{\ell}(1) \frac{2\ell+1}{2} P_{\ell} P_k d\mu, \end{aligned}$$

where

$$\sigma_{tk}^m = \sigma_t^m + \sigma_{sk}^m, \quad \text{and} \quad \sigma_{sk}^m = 2\pi \sigma_s \int_{-1}^1 P_k(\mu) s(\mu) d\mu.$$

3.3. Full discretization

To approximate the solution of the P_N equations in the spatial domain we introduce a continuous and piecewise linear finite element approximation space of dimension N_h for the coefficient functions $\psi_l(x)$ and $q_l(x)$ in the expansion. These spaces are closed finite subspaces of \mathcal{X} and Y , and defined as $\mathcal{X}_h := \mathcal{X}_{h,N}^+ \oplus \mathcal{X}_{h,N}^-$ and $\mathcal{Y}_h \in Y$ respectively, where

$$\begin{aligned}\mathcal{X}_{h,N}^+ &:= \{\psi_{\ell,i} : \psi(x, \mu) = \sum_{\ell=0}^N \sum_{i=0}^{N_h} \psi_{2\ell}^i \frac{4\ell+1}{2} P_{2\ell}(\mu) H_i(x)\}, \\ \mathcal{X}_{h,N}^- &:= \{\psi_{\ell,i} : \psi(x, \mu) = \sum_{\ell=0}^N \sum_{i=0}^{N_h} \psi_{2\ell+1}^i \frac{4\ell+3}{2} P_{2\ell+1}(\mu) H_i(x)\}.\end{aligned}$$

Here, $H_i(x)$ are the usual one-dimensional hat functions. Note that we employ the same finite element space for both even $\psi_{2\ell}(x)$ and odd $\psi_{2\ell+1}(x)$ components. The finite element approximation of the P_N equation serves as our “truth” approximation, i.e., we build the reduced basis approximation upon this P_N -FE approximation and shall measure the error with respect to the solution of the P_N -FE approximation.

Using this discretization, we obtain fully discrete optimality conditions. Given a parameter $p \in \mathcal{P}$, the truth optimal solution $(\psi_h^*, \lambda_h^*, q_h^*) \in \mathcal{X}_h \times \mathcal{X}_h \times \mathcal{Y}_h$ satisfies

$$a(\psi_h^*, \phi_h; p) = b(q_h^*, \phi_h; p), \quad \forall \phi_h \in \mathcal{X}_h, \quad (3.11a)$$

$$a(\phi_h, \lambda_h^*; p) = (\alpha(\bar{D} - \mathcal{L}\psi_h^*), \mathcal{L}\phi_h)_{Y(p)}, \quad \forall \phi_h \in \mathcal{X}_h, \quad (3.11b)$$

$$(q_h^*, \varphi_h)_{Y(p)} - b(\varphi_h, \lambda_h^*; p) = 0 \quad \forall \varphi_h \in \mathcal{Y}_h, \quad (3.11c)$$

The optimality system is dimension of $(2N+1)N_h + N_h$, where N_h is the FE dimension, and N is number of terms in P_N expansion.

Remark 3.1. We note that the fully discrete problem inherits the stability from the continuous setting since we have $\mathcal{A}\psi_h^+ \in \mathcal{X}_h^-$ for every $\psi_h^+ \in \mathcal{X}_h^+$. The discrete inf-sup condition

$$\beta_h(p) = \inf_{\psi_h \in \mathcal{X}_h} \sup_{\phi_h \in \mathcal{X}_h} \frac{a(\psi_h, \phi_h; p)}{\|\psi_h\|_{\mathcal{X}} \|\phi_h\|_{\mathcal{X}}} > 0 \quad (3.12)$$

thus holds for the FE- P_1 approximation with the same constant as for the continuous problem; see Ref. 15 for details.

Remark 3.2. From the definition of the Legendre polynomials it directly follows that

$$\int_{-1}^1 \psi(x, \mu) d\mu = \int_{-1}^1 \psi(x) P_0(\mu) d\mu = \psi_0(x). \quad (3.13)$$

Therefore, $\mathcal{L}\psi(x, \mu) = \psi_0(x)$.

4. Reduced Basis Approximation

We now turn to the RB method. We consider the RB approximation of the truth optimality system (3.11) in this section and develop associated rigorous a posteriori error bounds in the next section.

To this end, we assume that we are given the integrated reduced basis spaces

$$\mathcal{X}_{\mathcal{N}} = \text{span}\{\eta_n, 1 \leq n \leq \mathcal{N}\}, \quad 1 \leq \mathcal{N} \leq \mathcal{N}_{\max}, \quad (4.1)$$

where the η_n , $1 \leq n \leq \mathcal{N}$, are mutually $(\cdot, \cdot)_{\mathcal{X}}$ -orthogonal basis functions. Furthermore, we assume that the reduced basis control spaces are given by

$$\mathcal{Y}_{\mathcal{M}} = \text{span}\{\xi_m, 1 \leq m \leq \mathcal{M}\}, \quad 1 \leq \mathcal{M} \leq \mathcal{M}_{\max}, \quad (4.2)$$

where the ξ_m , $1 \leq m \leq \mathcal{M}$, are mutually $(\cdot, \cdot)_Y$ -orthogonal basis functions. In this work, we consider the proper orthogonal decomposition (POD) to generate these spaces: Let $\text{POD}_{\mathcal{X}}(\{v_k \in \mathcal{X} : 1 \leq k \leq n_{\text{train}}\}, \mathcal{N})$ return the \mathcal{N} largest POD modes with respect to the $(\cdot, \cdot)_{\mathcal{X}}$ inner product (and normalized with respect to the \mathcal{X} -norm) and $\text{POD}_Y(\{v_k \in Y : 1 \leq k \leq n_{\text{train}}\}, \mathcal{M})$ return the \mathcal{M} largest POD modes with respect to the $(\cdot, \cdot)_Y$ inner product (and normalized with respect to the Y -norm). We then define a finite but suitably large parameter train set $\Xi_{\text{train}} \subset \mathcal{P}$ of size n_{train} and define

$$\mathcal{X}_{\mathcal{N}_{\max}} = \text{POD}_{\mathcal{X}}(\{\psi^*(p) \in \mathcal{X}_h, \lambda^*(p) \in \mathcal{X}_h : p \in \Xi_{\text{train}}\}, \mathcal{N}_{\max}) \quad (4.3)$$

and

$$\mathcal{Y}_{\mathcal{M}_{\max}} = \text{POD}_Y(\{q^*(p) \in \mathcal{Y}_h : p \in \Xi_{\text{train}}\}, \mathcal{M}_{\max}), \quad (4.4)$$

where $\mathcal{N}_{\max} = 2(N+1)\mathcal{M}_{\max}$; in particular, $\mathcal{N}_{\max} = 4M_{\max}$ for the P_1 expansion. We note that the generation of the POD basis requires n_{train} solutions of the truth optimality system (3.11) and that the primal and dual solutions are integrated in the space $\mathcal{X}_{\mathcal{N}}$. Also note, however, that one could also employ the Greedy sampling procedure discussed in Ref. 28 to generate $\mathcal{X}_{\mathcal{N}}$ and $\mathcal{Y}_{\mathcal{M}}$.

4.1. Galerkin Projection

We next replace the truth approximation of the PDE constraint in (3.5) by its reduced basis approximation. The reduced basis optimal control problem is thus given by

$$\begin{aligned} \min_{\psi_{\mathcal{N}} \in \mathcal{X}_{\mathcal{N}}, q_{\mathcal{M}} \in \mathcal{Y}_{\mathcal{M}}} J(\psi_{\mathcal{N}}, q_{\mathcal{M}}; p) &= \frac{1}{2} \int_{\mathcal{I}(p)} \alpha (\mathcal{L}\psi_{\mathcal{N}} - \bar{D})^2 dx + \frac{1}{2} \int_{\mathcal{I}(p)} q_{\mathcal{M}}^2 dx \\ \text{s.t. } (\psi_{\mathcal{N}}, q_{\mathcal{M}}) \in \mathcal{X}_{\mathcal{N}} \times \mathcal{Y}_{\mathcal{M}} &\text{ solves } a(\psi_{\mathcal{N}}, \phi; p) = b(q_{\mathcal{M}}, \phi; p), \forall \phi \in \mathcal{X}_{\mathcal{N}}. \end{aligned} \quad (4.5)$$

We can also directly state the associated first-order optimality system: For a given parameter $p \in \mathcal{P}$, the optimal solution $(\psi_{\mathcal{N}}^*, \lambda_{\mathcal{N}}^*, q_{\mathcal{M}}^*) \in \mathcal{X}_{\mathcal{N}} \times \mathcal{X}_{\mathcal{N}} \times \mathcal{Y}_{\mathcal{M}}$ satisfies the

system of equations

$$a(\psi_{\mathcal{N}}^*, \phi; p) = b(q_{\mathcal{M}}^*, \phi; p), \quad \forall \phi \in \mathcal{X}_{\mathcal{N}}, \quad (4.6a)$$

$$a(\phi, \lambda_{\mathcal{N}}^*; p) = (\alpha(\bar{D} - \mathcal{L}\psi_{\mathcal{N}}^*), \mathcal{L}\phi)_{Y(p)}, \quad \forall \phi \in \mathcal{X}_{\mathcal{N}}, \quad (4.6b)$$

$$(q_{\mathcal{M}}^*, \varphi)_{Y(p)} - b(\varphi, \lambda_{\mathcal{N}}^*; p) = 0, \quad \forall \varphi \in Y_{\mathcal{M}}. \quad (4.6c)$$

The reduced basis optimality system is only of dimension $2\mathcal{N} + \mathcal{M}$ and can be evaluated efficiently using an offline-online computational decomposition. We refer to Ref. 28 for details, where the computational procedure including computational costs are discussed.

Remark 4.1. We note that the standard Galerkin projection considered for the state and adjoint equations in (4.6) does not guarantee the stability of the reduced basis approximation, i.e., $\beta_h(p) > 0$ in (3.12) does not generally imply that $\beta_{\mathcal{N}}(p) > 0$, where

$$\beta_{\mathcal{N}}(p) = \inf_{\psi \in \mathcal{X}_{\mathcal{N}}} \sup_{\phi \in \mathcal{X}_{\mathcal{N}}} \frac{a(\psi_{\mathcal{N}}, \phi_{\mathcal{N}}; p)}{\|\psi_{\mathcal{N}}\|_{\mathcal{X}} \|\phi_{\mathcal{N}}\|_{\mathcal{X}}} \quad (4.7)$$

is the inf-sup constant associated with the reduced basis approximation. More sophisticated approaches, e.g. enriching the test space with supremizer functions and employing a Petrov-Galerkin approximation, do restore guaranteed stability at some additional complexity and cost^{41,35}. In this paper, however, we will consider only the standard Galerkin approach and verify the stability numerically. To this end, we compute the inf-sup constant (4.7) for 100 randomly chosen parameter values $p \in \Xi_{\text{test}}$ (see Table 2) and different RB dimensions \mathcal{N} . We present the minimum value for different \mathcal{N} in Table 1, showing that $\beta_{\mathcal{N}}(p) > 0$ is indeed satisfied. Note that the minimum inf-sup constant of the P_1 - FE approximation is $\beta_h(p) = 3.3323$, and thus $\beta_{\mathcal{N}}(p)$ is very close to $\beta_h(p)$ for $\mathcal{N} \geq 25$. Finally, we recall that using integrated spaces for the state and adjoint preserves the stability of the optimality system²⁰.

\mathcal{N}	5	10	15	25	35
$\min_{p \in \mathcal{P}_{\text{ex}}} \beta_{\mathcal{N}}(p)$	3.0183	3.258	3.321	3.3323	3.3323

Table 1: Minimum inf-sup constants $\beta_{\mathcal{N}}(p)$ over Ξ_{test} for various values of \mathcal{N} .

5. A Posteriori Error Estimation

We turn to the *a posteriori* error estimation procedure. We follow the ideas presented in Ref. 28 and extend the bound introduced there to the radiation treatment planning problem.

To begin, we assume that we are given a positive lower bound $\beta_{LB}(p) : \mathcal{P} \rightarrow \mathbb{R}$ for the inf-sup constant $\beta_h(p) > 0$ defined in (3.12). Furthermore, we assume that we have upper bounds available for the (parameter-dependent) constant

$$\gamma_{\mathcal{L}}^{\text{UB}}(p) \geq \|\mathcal{L}\|_{\mathcal{X} \rightarrow Y(p)} := \sup_{\phi \in \mathcal{X}} \frac{\|\mathcal{L}\phi\|_{Y(p)}}{\|\phi\|_{\mathcal{X}}}, \quad (5.1)$$

and the continuity constant of the bilinear form $b(\cdot, \cdot; p)$

$$\gamma_b^{\text{UB}}(p) \geq \gamma_b(p) := \sup_{\psi \in \mathcal{Y}_h} \sup_{\phi \in \mathcal{X}_h} \frac{b(\psi, \phi; p)}{\|\psi\|_{Y(p)} \|\phi\|_{\mathcal{X}}} > 0, \quad \forall p \in P. \quad (5.2)$$

We also define the state, adjoint, and control optimality errors as $e^\psi(p) = \psi_h^*(p) - \psi_{\mathcal{N}}^*(p)$, $e^\lambda(p) = \lambda_h^*(p) - \lambda_{\mathcal{N}}^*(p)$, and $e^q(p) = q_h^*(p) - q_{\mathcal{M}}^*(p)$, respectively. In the following we often drop the dependence on p to simplify notation.

5.1. Error Bound for Optimal Control

We obtain the following result for the error in the optimal control.

Proposition 5.1. *Let q_h^* and $q_{\mathcal{M}}^*$ be the optimal solutions to the truth and reduced basis optimal control problem, respectively. The error in the optimal control satisfies for all parameters $p \in \mathcal{P}$*

$$\begin{aligned} \|q_h^* - q_{\mathcal{M}}^*\|_{Y(p)} &\leq \Delta_{\mathcal{M}}^q(p) \equiv \frac{1}{2} \left(\|r_q(\cdot; p)\|_{Y(p)'} + \frac{\gamma_b^{\text{UB}}(p)}{\beta_{LB}(p)} \|r_\lambda(\cdot; p)\|_{\mathcal{X}'} \right) \\ &+ \frac{1}{2} \left[\left(\frac{8}{\beta_{LB}(p)} \|r_\psi(\cdot; p)\|_{\mathcal{X}'} \|r_\lambda(\cdot; p)\|_{\mathcal{X}'} + \frac{\|\sqrt{\alpha}\|_{L^\infty(\mathcal{I})}^2 \gamma_{\mathcal{L}}^{\text{UB}}(p)^2}{\beta_{LB}(p)^2} \|r_\psi(\cdot; p)\|_{\mathcal{X}'}^2 \right) \right. \\ &\quad \left. + \left(\|r_q(\cdot; p)\|_{Y(p)'} + \frac{\gamma_b^{\text{UB}}(p)}{\beta_{LB}(p)} \|r_\lambda(\cdot; p)\|_{\mathcal{X}'} \right)^2 \right]^{\frac{1}{2}} \end{aligned} \quad (5.3)$$

Proof. We first note that the state error satisfies the error residual equation

$$a(e^\psi, \phi; p) = r_\psi(\phi; p) + b(e^q, \phi; p), \quad \forall \phi \in \mathcal{X}_h, \quad (5.4)$$

where the residual of the state equation is given by $r_\psi(\phi, p) = b(q_{\mathcal{M}}^*, \phi, p) - a(\psi_{\mathcal{N}}^*, \phi, p)$, $\forall \phi \in \mathcal{X}_h$. Choosing $\phi = T_p e^\psi$ as test function in (5.4), where the supremizer $T_p : \mathcal{X}_h \rightarrow \mathcal{X}_h$ is given by $(T_p w, \phi)_{\mathcal{X}} = a(w, \phi; p)$, $\forall \phi \in \mathcal{X}_h$, we obtain

$$\beta_{LB}(p) \|T_p e^\psi\|_{\mathcal{X}} \|e^\psi\|_{\mathcal{X}} \leq a(e^\psi, T_p e^\psi; p) = r_\psi(T_p e^\psi; p) + b(e^q, T_p e^\psi; p).$$

Invoking (5.2) it follows that

$$\|e^\psi\|_{\mathcal{X}} \leq \frac{1}{\beta_{LB}(p)} (\|r_\psi(\cdot; p)\|_{\mathcal{X}'} + \gamma_b^{\text{UB}}(p) \|e^q\|_{Y(p)}). \quad (5.5)$$

Similarly, we note that the adjoint error satisfies the error residual equation

$$a(\phi, e^\lambda; p) = r_\lambda(\phi; p) - (\alpha \mathcal{L} e^\psi, \mathcal{L} \phi)_{Y(p)}, \quad \forall \phi \in \mathcal{X}_h, \quad (5.6)$$

16 *B. Ahmedov, M.A. Grepl, M. Herty*

where the adjoint residual is given by $r_\lambda(\phi, p) = (\alpha(\bar{D} - \mathcal{L}\psi_{\mathcal{N}}^*), \mathcal{L}\phi)_{Y(p)} - a(\phi, \lambda_{\mathcal{N}}^*; p)$, $\forall \phi \in \mathcal{X}_h$. Choosing as test function $\phi = T_p e^\lambda$ in (5.6) and noting from (5.1) and the Cauchy-Schwarz Inequality that

$$(\alpha \mathcal{L} e^\psi, \mathcal{L} T_p e^\lambda)_{Y(p)} \leq \|\sqrt{\alpha}\|_{L^\infty(\mathcal{I})} \gamma_{\mathcal{L}}^{\text{UB}}(p) \|\sqrt{\alpha} \mathcal{L} e^\psi\|_{Y(p)} \|T_p e^\lambda\|_{\mathcal{X}} \quad (5.7)$$

we arrive at

$$\|e^\lambda\|_{\mathcal{X}} \leq \frac{1}{\beta_{\text{LB}}(p)} (\|r_\lambda(\cdot; p)\|_{\mathcal{X}'} + \|\sqrt{\alpha}\|_{L^\infty(\mathcal{I})} \gamma_{\mathcal{L}}^{\text{UB}}(p) \|\sqrt{\alpha} \mathcal{L} e^\psi\|_{Y(p)}). \quad (5.8)$$

We next note that the error in the optimal control satisfies

$$(e^q, \varphi)_{Y(p)} - b(\varphi, e^\lambda; p) = r_q(\varphi; p), \quad \forall \varphi \in \mathcal{Y}_h, \quad (5.9)$$

where the residual is given by $r_q(\varphi, p) = b(\varphi, \lambda_{\mathcal{N}}^*; p) - (q_{\mathcal{M}}^*, \varphi)_{Y(p)}$, $\forall \varphi \in \mathcal{Y}_h$. We choose as test functions $\phi = e^\lambda$ in (5.4), $\phi = e^\psi$ in (5.6), and $\varphi = e^q$ in (5.9) and obtain

$$a(e^\psi, e^\lambda; p) - b(e^q, e^\lambda; p) = r_\psi(e^\lambda; p), \quad (5.10)$$

$$a(e^\psi, e^\lambda; p) + (\alpha \mathcal{L} e^\psi, \mathcal{L} e^\psi)_{Y(p)} = r_\lambda(e^\psi; p), \quad (5.11)$$

$$(e^q, e^q)_{Y(p)} - b(e^q, e^\lambda; p) = r_q(e^q; p). \quad (5.12)$$

Adding (5.12) and (5.11) and subtracting (5.10) yields

$$(e^q, e^q)_{Y(p)} + (\alpha \mathcal{L} e^\psi, \mathcal{L} e^\psi)_{Y(p)} = -r_\psi(e^\lambda; p) + r_\lambda(e^\psi; p) + r_q(e^q; p) \quad (5.13)$$

and hence

$$\begin{aligned} \|e^q\|_{Y(p)}^2 + \|\sqrt{\alpha} \mathcal{L} e^\psi\|_{Y(p)}^2 &\leq \|r_\psi(\cdot; p)\|_{\mathcal{X}'} \|e^\lambda\|_{\mathcal{X}} + \|r_\lambda(\cdot; p)\|_{\mathcal{X}'} \|e^\psi\|_{\mathcal{X}} + \\ &\quad + \|r_q(\cdot; p)\|_{Y(p)'} \|e^q\|_{Y(p)}. \end{aligned} \quad (5.14)$$

By substituting (5.5) and (5.8) into (5.14) we obtain

$$\begin{aligned} \|e^q\|_{Y(p)}^2 + \|\sqrt{\alpha} \mathcal{L} e^\psi\|_{Y(p)}^2 &\leq \|r_q(\cdot; p)\|_{Y(p)'} \|e^q\|_{Y(p)} \\ &\quad + \|r_\psi(\cdot; p)\|_{\mathcal{X}'} \frac{1}{\beta_{\text{LB}}(p)} (\|r_\lambda\|_{\mathcal{X}'} + \|\sqrt{\alpha}\|_{L^\infty(\mathcal{I})} \gamma_{\mathcal{L}}^{\text{UB}}(p) \|\sqrt{\alpha} \mathcal{L} e^\psi\|_{Y(p)}) \\ &\quad + \|r_\lambda(\cdot; p)\|_{\mathcal{X}'} \frac{1}{\beta_{\text{LB}}(p)} (\|r_\psi\|_{\mathcal{X}'} + \gamma_b^{\text{UB}}(p) \|e^q\|_{Y(p)}). \end{aligned}$$

Furthermore, it follows from Young's inequality that

$$\begin{aligned} \frac{\|\sqrt{\alpha}\|_{L^\infty(\mathcal{I})} \gamma_{\mathcal{L}}^{\text{UB}}(p)}{\beta_{\text{LB}}(p)} \|r_\psi(\cdot; p)\|_{\mathcal{X}'} \|\sqrt{\alpha} \mathcal{L} e^\psi\|_{Y(p)} &\leq \\ \frac{\|\sqrt{\alpha}\|_{L^\infty(\mathcal{I})}^2 \gamma_{\mathcal{L}}^{\text{UB}}(p)^2}{4\beta_{\text{LB}}(p)^2} \|r_\psi(\cdot; p)\|_{\mathcal{X}'}^2 + \|\sqrt{\alpha} \mathcal{L} e^\psi\|_{Y(p)}^2. \end{aligned}$$

By combining the last two equations we obtain

$$\begin{aligned} \|e^q\|_{Y(p)}^2 &\leq \|r_q(\cdot; p)\|_{Y(p)'} \|e^q\|_{Y(p)} + \frac{2}{\beta_{LB}(p)} \|r_\psi(\cdot; p)\|_{\mathcal{X}'} \|r_\lambda(\cdot; p)\|_{\mathcal{X}'} + \\ &\quad + \frac{\gamma_b^{UB}(p)}{\beta_{LB}(p)} \|r_\lambda(\cdot; p)\|_{\mathcal{X}'} \|e^q\|_{Y(p)} + \frac{\|\sqrt{\alpha}\|_{L^\infty(\mathcal{I})}^2 \gamma_{\mathcal{L}}^{UB}(p)^2}{4\beta_{LB}(p)^2} \|r_\psi(\cdot; p)\|_{\mathcal{X}'}^2, \end{aligned}$$

This can be written in the form of a quadratic inequality for $\|e^q\|_{Y(p)}$ by

$$A\|e^q\|_{Y(p)}^2 + B\|e^q\|_{Y(p)} + C \leq 0 \quad (5.15)$$

where

$$\begin{aligned} A &= 1 \\ B &= - \left(\|r_q(\cdot; p)\|_{Y(p)'} + \frac{\gamma_b^{UB}(p)}{\beta_{LB}} \|r_\lambda(\cdot; p)\|_{\mathcal{X}'} \right) \\ C &= - \left(\frac{2}{\beta_{LB}(p)} \|r_\psi(\cdot; p)\|_{\mathcal{X}'} \|r_\lambda(\cdot; p)\|_{\mathcal{X}'} + \frac{\|\sqrt{\alpha}\|_{L^\infty(\mathcal{I})}^2 \gamma_{\mathcal{L}}^{UB}(p)^2}{4\beta_{LB}(p)^2} \|r_\psi(\cdot; p)\|_{\mathcal{X}'}^2 \right) \end{aligned}$$

which is satisfied iff

$$\Delta_{\mathcal{N}}^- \leq \|e^q\|_{Y(p)} \leq \Delta^+ \quad \text{with} \quad \Delta^\pm = \frac{-B \pm \sqrt{B^2 - 4AC}}{2A}.$$

The result follows by setting $\Delta_{\mathcal{N}}^q(p) = \Delta_{\mathcal{N}}^+$. \square

5.2. Error Bound for Cost Functional

Given the error bound for the optimal control we may readily derive a bound for the error in the cost functional. To this end, we follow the approach described in Ref. 28 and first derive a bound for the optimality error in the state and adjoint solution.

Lemma 5.1. *The state optimality error, $e^\psi = \psi^* - \psi_{\mathcal{N}}^*$, is bounded by*

$$\|e^\psi\|_{\mathcal{X}} \leq \Delta_{\mathcal{N}}^\psi(p) = \frac{1}{\beta_{LB}(p)} (\|r_\psi(\cdot; p)\|_{\mathcal{X}'} + \gamma_b^{UB}(p) \Delta_{\mathcal{M}}^q(p)), \quad \forall p \in \mathcal{P} \quad (5.16)$$

Proof. The proof follows from the inequality (5.5) and Proposition 5.1. \square

Lemma 5.2. *The adjoint optimality error, $e^\lambda = \lambda^* - \lambda_{\mathcal{N}}^*$, is bounded by*

$$\|e^\lambda\|_{\mathcal{X}} \leq \Delta_{\mathcal{N}}^\lambda(p) = \frac{1}{\beta_{LB}(p)} (\|r_\lambda(\cdot; p)\|_{\mathcal{X}'} + \|\alpha\|_{L^\infty(\mathcal{I})} \gamma_{\mathcal{L}}^{UB}(p)^2 \Delta_{\mathcal{N}}^\psi(p)), \quad \forall p \in \mathcal{P} \quad (5.17)$$

Proof. We follow the same steps leading to inequality (5.8), but note that

$$(\alpha \mathcal{L} e^\psi, \mathcal{L} T_p e^\lambda)_{Y(p)} \leq \|\alpha\|_{L^\infty(\mathcal{I})} \gamma_{\mathcal{L}}^{UB}(p)^2 \|e^\psi\|_{\mathcal{X}} \|T_p e^\lambda\|_{\mathcal{X}}. \quad (5.18)$$

The result then follows by invoking Lemma 5.1 to bound $\|e^\psi\|_{\mathcal{X}}$. \square

The error in the cost functional can thus be estimated as follows.

Proposition 5.2. *Let $J^* = J(\psi^*, q^*; p)$ and $J_{\mathcal{N}}^* = J(\psi_{\mathcal{N}}^*, q_{\mathcal{N}}^*; p)$ be the optimal cost functional value for the truth and RB solutions. The error then satisfies*

$$|J^* - J_{\mathcal{N}}^*| \leq \Delta_{\mathcal{N}}^J(p) = \frac{1}{2} \left(\|r_{\psi}(\cdot; p)\|_{\mathcal{X}'} \Delta_{\mathcal{N}}^{\lambda}(p) + \|r_{\lambda}(\cdot; p)\|_{\mathcal{X}'} \Delta_{\mathcal{N}}^{\psi}(p) + \|r_q(\cdot; p)\|_{Y(p)'} \Delta_{\mathcal{M}}^q(p) \right), \quad \forall p \in \mathcal{P} \quad (5.19)$$

Proof. We use the standard result from Ref. 5 to bound the cost functional error by

$$\begin{aligned} |J^* - J_{\mathcal{N}}^*| &= \frac{1}{2} (r_{\psi}(e^{\lambda}; p) + r_{\lambda}(e^{\psi}; p) + r_q(e^q; p)) \\ &\leq \frac{1}{2} (\|r_{\psi}(\cdot; p)\|_{\mathcal{X}'} \|e^{\lambda}\|_{\mathcal{X}} + \|r_{\lambda}(\cdot; p)\|_{\mathcal{X}'} \|e^{\psi}\|_{\mathcal{X}} \\ &\quad + \|r_q(\cdot; p)\|_{Y(p)'} \|e^q\|_{Y(p)}), \quad \forall p \in \mathcal{P}. \end{aligned}$$

The result follow from Lemma 5.1 and 5.2 and Proposition 5.1. \square

5.3. Computational Procedure

The evaluation of the control and cost functional error bound requires computation of

- (1) the dual norms of the state, adjoint, and optimality equation residuals $\|r_{\psi}(\cdot; p)\|_{\mathcal{X}'}$, $\|r_{\lambda}(\cdot; p)\|_{\mathcal{X}'}$, and $\|r_q(\cdot; p)\|_{Y(p)'}$; respectively; and
- (2) the constants $\beta_{\text{LB}}(p)$, $\gamma_{\mathcal{L}}^{\text{UB}}(p)$, and $\gamma_b^{\text{UB}}(p)$.

All of these quantities can be computed using an offline-online decomposition. Since the approach is more or less standard, we do not present the details here but refer to Ref. 34 for details concerning the dual norms of the state and adjoint residuals and to Ref. 28 for the remaining quantities. We note, however, that the online computational complexity to evaluate all involved quantities depends only on the dimension of the reduced spaces and is *independent* of the dimension of the underlying truth approximation.

6. Numerical Results

We present a numerical example to confirm the validity of the proposed approach. The numerical schemes have been implemented in MATLAB[®] and are available online¹. The source package is designed such that different examples do not require changes in the solvers (`solver.m`, `RB_solver.m`). For each example a separate file is created (e.g. `ex_forw_constMat.m`) which defines the problem and executes the solver. Example files and solvers (and also various functions) employ a MATLAB[®] struct `par` where the problem parameters are stored, e.g., the problem

name (`par.name`), definition of functions for material parameters (`par.sigma_a`, `par.sigma_sm`), profile of a dose distribution (`par.dose`) and so on; we refer to Ref. 1 for more details.

6.1. Model Problem

For our model problem we consider the parametrized geometry introduced in Section 3.1 and sketched in Figure 1. The admissible range \mathcal{P}_1 to \mathcal{P}_4 of the four geometry parameters p_1 to p_4 are summarized in Table 2, with the full parameter domain given by $\mathcal{P} = \mathcal{P}_1 \times \mathcal{P}_2 \times \mathcal{P}_3 \times \mathcal{P}_4$. We choose as reference parameter $\bar{p} = [0.2; 0.07; 0.8; 0.07]$. The absorption coefficient σ_a , scattering cross-section σ_s , and total cross-section $\sigma_t = \sigma_a + \sigma_s$ are assumed piece-wise constant in the five subdomains introduced in Section 3.1 and are also given in Table 2.

We assume that the tumor is located in the subdomain $\Omega_T = [0.38, 0.62]$ of the reference domain, i.e., we also allow the tumor to be changing in size with the parameters. The desired dose should be maximal in the tumor region and negligibly small in the other areas. We therefore set the desired dose as sketched in Fig. 2. We set the regularization parameter $\alpha = 10$ over the whole domain.

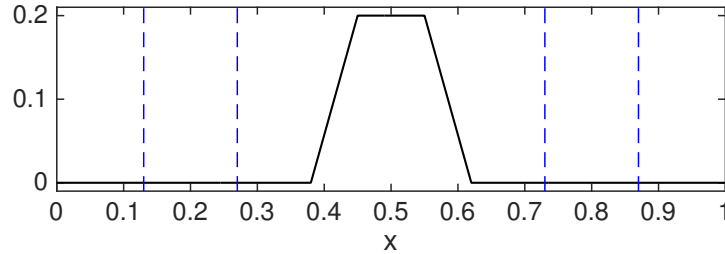


Fig. 2: Profile of parametrized desired dose $\bar{\psi}(x)$ in reference geometry Ω .

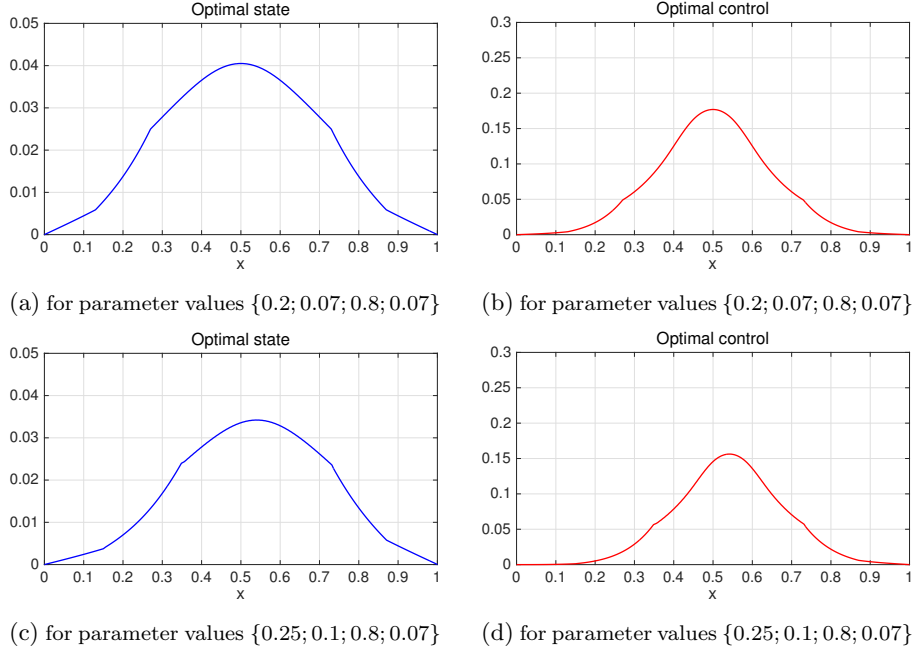
For the truth discretization we employ a piece-wise linear finite element approximation space for the state, adjoint, and control variables. The number of degrees of freedom is $\dim(\mathcal{X}_h) = \dim(\mathcal{Y}_h) = N_h = 200$. The total dimension of the truth optimality system is thus $5N_h = 1000$. In Fig. 3 we present sample solutions for the optimal state and control for two parameter values.

We construct the reduced basis spaces $\mathcal{Y}_{\mathcal{M}}$ and $\mathcal{X}_{\mathcal{N}}$ according to the POD procedure described in Section 4. For this purpose, we employ the train sample $\Xi_{\text{train}} = \mathcal{P}_1^{\text{train}} \times \mathcal{P}_2^{\text{train}} \times \mathcal{P}_3^{\text{train}} \times \mathcal{P}_4^{\text{train}}$ consisting of $n_{\text{train}} = 324$ equidistant parameter points over \mathcal{P} . We also introduce a parameter test sample Ξ_{test} of size $n_{\text{test}} = 100$ with a uniform-random distribution in \mathcal{P} . The model problem for these parameters is implemented in the example file `ex_optim.pDose_constMat.m`.

20 *B. Ahmedov, M.A. Grepl, M. Herty*

N_h	200	\mathcal{P}_1	[0.15 ; 0.25]
Ω_T	[0.38, 0.62]	\mathcal{P}_2	[0.04 ; 0.1]
Ω_N	$(0.1, 0.38) \times (0.62, 0.9)$	\mathcal{P}_3	[0.15 ; 0.25]
Ω_R	$[0, 0.1] \times [0.9, 1]$	\mathcal{P}_4	[0.04 ; 0.1]
α	10	$\mathcal{P}_1^{\text{train}}$	[0.15; 0.17; 0.19; 0.21; 0.23; 0.25]
$\sigma_a^{1,\dots,5}$	[4; 7; 4; 7; 4]	$\mathcal{P}_2^{\text{train}}$	[0.04; 0.07; 0.10]
$\sigma_s^{1,\dots,5}$	[1; 2; 1; 2; 1]	$\mathcal{P}_3^{\text{train}}$	[0.75; 0.77; 0.79; 0.81; 0.83; 0.85]
\bar{p}	[0.2; 0.07; 0.8; 0.07]	$\mathcal{P}_4^{\text{train}}$	[0.04; 0.07; 0.10]
Ξ_{test}	100 random parameters	Ξ_{train}	$\mathcal{P}_1^{\text{train}} \times \mathcal{P}_2^{\text{train}} \times \mathcal{P}_3^{\text{train}} \times \mathcal{P}_4^{\text{train}}$

Table 2: Parameters for the numerical example.

Fig. 3: Zero-th moments of optimal state $\psi_0^*(x)$ and optimal control $q_0^*(x)$ for various parameter values with constant regularization parameter $\alpha = 10$ in the original geometry $\Omega_0(p)$.

6.2. Error Estimators

We first consider the performance of the *a posteriori* error bounds. We use a global upper bound for the (parameter-dependent) constants $\gamma_{\mathcal{L}}^{\text{UB}}(p)$ defined in (5.1) and $\gamma_b^{\text{UB}}(p)$ defined in (5.2). To this end, we compute the values for $\|\mathcal{L}\|_{\mathcal{X} \rightarrow Y(p)}$ and $\gamma_b(p)$ over the training set Ξ_{test} to find that $\|\mathcal{L}\|_{\mathcal{X} \rightarrow Y(p)}$ varies in the range 1.02

to 1.271 and $\gamma_b(p)$ varies from 1.04 to 1.615; we therefore set $\gamma_{\mathcal{L}}^{\text{UB}}(p) = 1.271$ and $\gamma_b^{\text{UB}}(p) = 1.615$. For the inf-sup lower bound $\beta_{\text{LB}}(p)$ we also use the global lower bound $\beta_{\text{LB}}(p) = 3.3323$ given by the minimum value of $\beta_h(p)$ over Ξ_{test} ; also see Remark 4.1. We are aware that these upper and lower bounds are not guaranteed to hold for all $p \in \mathcal{P}$. However, since the performance of the error bounds is tested on Ξ_{test} , we deem this approach to be sufficient for our study.

In Figure 4 we present, as a function of \mathcal{M} , the maximum absolute errors and error bounds for the optimal state and adjoint variable, the optimal control, and the associated cost functional. The errors and bounds are averaged over the test sample Ξ_{test} . We note that our *a posteriori* error bounds considerably overestimate the actual errors. We also note, however, the bound for the control and the cost become sharper as \mathcal{M} increases, with the effectivity for the control bound reaching $\mathcal{O}(10)$ for $\mathcal{M} = 50$. Given the exponential convergence of the reduced basis solution and the fact that for larger values of \mathcal{M} the error bounds are well below the acceptable tolerance, we consider the proposed bounds to be a useful tool to certify the reduced basis solution.

One reason for the overestimation of the state and adjoint error presumably lies in the transport character of the Boltzmann transport equation, where the pure Galerkin approximation does not yield a sufficiently tight relation between the error and the residual. In this context we also refer to Ref. 33, where similarly pessimistic reduced basis *a posteriori* bounds have been observed for a Boltzmann model problem. An attempt to improve the efficiency of the bounds based on ideas presented in Ref. 12 is a topic of future research.

The example file for the computation of the errors and error bounds is implemented in `ex_RBoptim_constMat.mRBspace.m`. The results and figures can be reproduced by running this file.

6.3. Uncertainty Quantification of Treatment Plans

We now turn to the efficient computation of the uncertainty in the treatment plan under geometric variations obtained from the patient's CT scan. We assume that the geometry parameters are not known precisely, but instead are random variables distributed by a normal distribution with a fixed mean and variance, i.e., $p_i \sim \mathcal{N}(\bar{p}_i, \sigma_i^2)$, $i = 1, \dots, 4$, where \bar{p}_i denotes the mean and σ_i^2 the variance.

We employ the reduced basis approximation in combination with a Monte Carlo simulation to quantify the uncertainty of the optimal treatment plan under parametric variations. More precisely, we compute the expected value of the optimal control, $\mathbb{E}(q^*(p))$, where p is drawn from $\mathcal{N}(\bar{p}_i, \sigma_i^2)$ using the MC simulation and compare the result with the optimal control for the mean parameter value, i.e., $q^*(\bar{p})$. We also compute the difference $|\mathbb{E}(q^*(p)) - q^*(\bar{p})|$ for different variances and plot the L^∞ - and L^2 -norm of the difference as a function of the variance. This allows to assess up to which noise level in the geometry data the optimal treatment plan is still reliable.

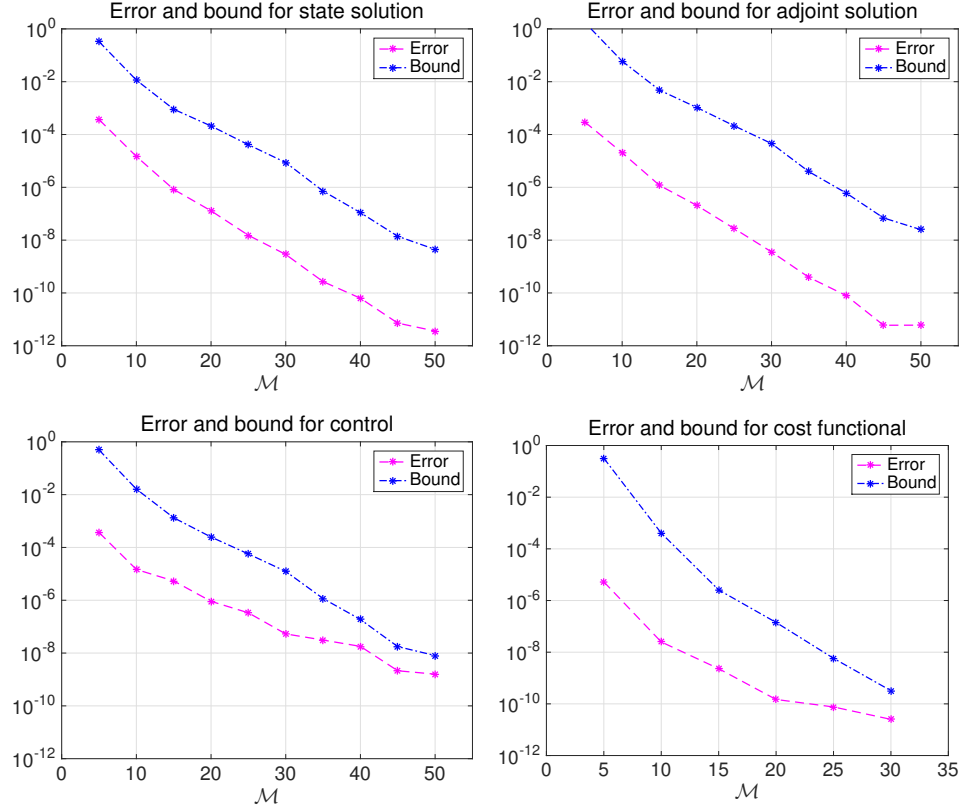


Fig. 4: Maximum errors and error bounds for state, adjoint, control and cost functional as a function of M .

We first keep $p_2 = p_4 = 0.07$ fixed and only consider variations in p_1 and p_3 . In Figure 5 on the left we plot the mean optimal control, i.e., the optimal control for the mean parameter values $\bar{p}_1 = 0.2$ and $\bar{p}_3 = 0.8$, and the expected value of the optimal control for the variances $\sigma = 0.04$ and 0.05 . In Figure 5 on the right we plot the difference between the mean and expected value in the L^∞ - and L^2 -norm over the variance. In Figure 6 we show analogous results for fixed $p_1 = 0.2$ and $p_3 = 0.8$ and varying in p_2 and p_4 and in Figure 7 for the case where all parameters are varying. In all cases we observe a close to linear dependence of the difference between the mean and expected value on the variance. We also observe that the uncertainty in p_2 and p_4 has a slightly larger effect on the optimal treatment plan than the uncertainty in p_1 and p_3 . The difference from the mean control (resp. treatment plan) of course occurs if all four parameter are uncertain.

In this study, we employed the reduced basis approximation only within the MC simulation to efficiently propagate and assess the uncertainty in the parameters. Future work will address the use of the *a posteriori* error bounds in the uncertainty

quantification, i.e., to also provide certified error bounds for the expected value of the optimal treatment plan.

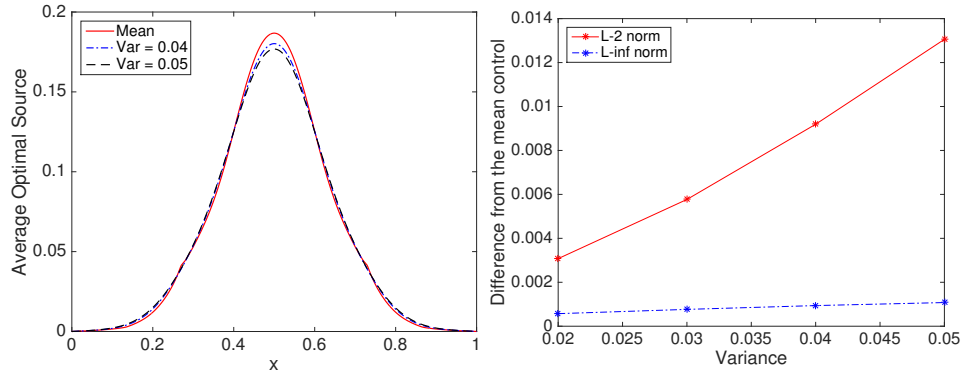


Fig. 5: Mean and expected value of optimal control over Ω (left) and the difference as a function of the variance (right) given uncertainty in p_1 and p_3 ; mean values $\bar{p}_1 = 0.2$ and $\bar{p}_3 = 0.8$; number of MC samples $n_{MC} = 10^5$.

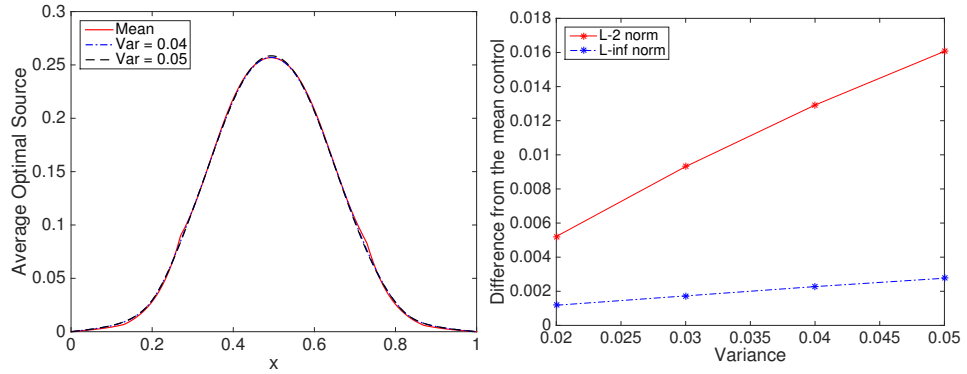


Fig. 6: Mean and expected value of optimal control over Ω (left) and the difference as a function of the variance (right) given uncertainty in p_2 and p_4 ; mean values $\bar{p}_2 = 0.07$ and $\bar{p}_4 = 0.07$; number of MC samples $n_{MC} = 10^5$.

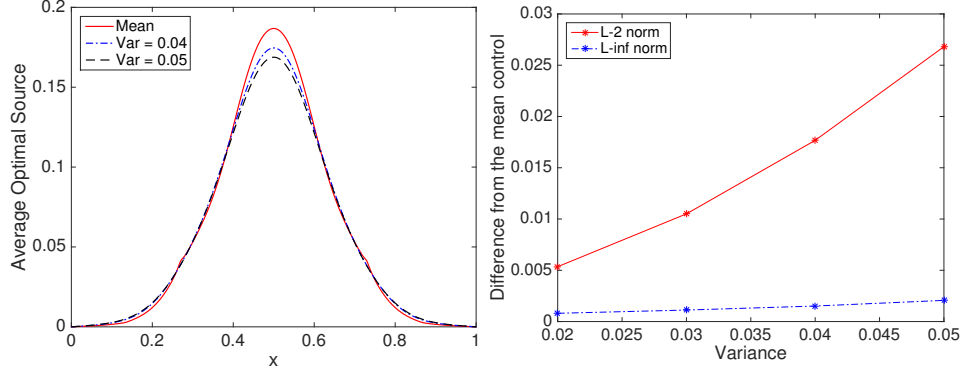
24 *B. Ahmedov, M.A. Grepl, M. Herty*

Fig. 7: Mean and expected value of optimal control over Ω (left) and the difference as a function of the variance (right) given uncertainty in p_1 , p_2 , p_3 , and p_4 ; mean values $\bar{p}_1 = 0.2$, $\bar{p}_2 = 0.07$, $\bar{p}_3 = 0.8$, and $\bar{p}_4 = 0.07$; number of MC samples $n_{\text{MC}} = 10^5$.

Appendix A. Geometric transformation and affine decomposition

We consider a one-dimensional parametrized slab geometry denoted by $\Omega_0(p)$. The parameters describe the center and halfwidth of the subdomain $\Omega_0^2(p)$ and $\Omega_0^4(p)$, we thus have four parameters $p = (p_1, p_2, p_3, p_4) \in \mathcal{P} \subset \mathbb{R}^4$. A sketch of the domain is shown in Figure 1. In order to derive an efficient offline-online computational decomposition, we require that the bilinear forms satisfy the affine parameter dependence (3.2) and (3.3), where $\theta_{a,b}^m : \mathcal{P} \rightarrow \mathbb{R}$ are parameter dependent functions and a^m and b^m are parameter independent bilinear and linear forms, respectively. We thus perform an affine mapping from the parameter dependent geometry $\Omega_0(p)$ to a parameter independent reference geometry Ω , see Ref. 34, 2 for details. Note that $\Omega = \Omega_0(\bar{p})$ for some fixed reference parameter \bar{p} . We recall the bilinear forms

$$b(q, \phi; p) = (q, \phi)_{\mathcal{I}(p)} = \int_{\Omega_0(p)} \int_{-1}^1 q \phi \, dx_0 \, d\mu, \quad (\text{A.1})$$

and

$$\begin{aligned} a(\psi, \phi; p) = & \int_{\Omega_0(p)} \int_{-1}^1 \mu (\phi^- \partial_{x_0} \psi^+ - \psi^- \partial_{x_0} \phi^+) \, dx_0 \, d\mu + \int_{\Omega_0(p)} \int_{-1}^1 \sigma_t \phi \psi \, dx_0 \, d\mu \\ & - \int_{\Omega_0(p)} \int_{-1}^1 \sigma_s \left\{ \int s(\mu, \mu') \phi(\mu') \, d\mu' \right\} \psi \, dx_0 \, d\mu + \sum_{x \in \{0,1\}} \int_{-1}^1 |\mu| \phi^+(x, \mu) \psi^+(x, \mu) \, d\mu. \end{aligned} \quad (\text{A.2})$$

where the integrals in space are performed over $\Omega_0(p)$. The affine mapping for $x \in \Omega^k$ is given by $x_0 = G^k(p)x + c^k(\mu)$ and the inverse mapping is thus $x = (G^k(\mu))^{-1}(x_0 - c^k(\mu))$ for $k = 1, \dots, 5$. We have $\frac{\partial x}{\partial x_0} = (G^k(\mu))^{-1}$ and $d\Omega_0(\mu) = |\det G(\mu)| d\Omega = |G(\mu)| d\Omega$. After mapping to the reference geometry we thus obtain

$Q_b = 5$ with

$$\begin{aligned}\theta_b^1(p) &= \frac{p_1 - p_2}{\bar{p}_1 - \bar{p}_2}, & \theta_b^2(p) &= \frac{p_2}{\bar{p}_2}, & \theta_b^3(p) &= \frac{p_3 - p_4 - p_1 - p_2}{\bar{p}_3 - \bar{p}_4 - \bar{p}_1 - \bar{p}_2}, \\ \theta_b^4(p) &= \frac{p_4}{\bar{p}_4}, & \theta_b^5(p) &= \frac{1 - p_3 - p_4}{1 - \bar{p}_3 - \bar{p}_4},\end{aligned}$$

and

$$b^m(\phi) = \int_{\Omega^m} \int_{-1}^1 q \phi \, dx \, d\mu, \quad m = 1, \dots, 5.$$

Similarly, we obtain the affine decomposition (3.2) for $Q_a = 6$ with

$$\begin{aligned}\theta_a^1(p) &= \frac{p_1 - p_2}{\bar{p}_1 - \bar{p}_2}, & \theta_a^2(p) &= \frac{p_2}{\bar{p}_2}, & \theta_a^3(p) &= \frac{p_3 - p_4 - p_1 - p_2}{\bar{p}_3 - \bar{p}_4 - \bar{p}_1 - \bar{p}_2}, \\ \theta_a^4(p) &= \frac{p_4}{\bar{p}_4}, & \theta_a^5(p) &= \frac{1 - p_3 - p_4}{1 - \bar{p}_3 - \bar{p}_4}, & \theta_a^6(p) &= 1,\end{aligned}$$

and

$$\begin{aligned}a^m(\psi, \phi) &= \int_{\Omega^m} \int_{-1}^1 \sigma_t \phi \psi \, dx \, d\mu - \int_{\Omega^m} \int_{-1}^1 \sigma_s \left\{ \int s(\mu, \mu') \phi(\mu') \, d\mu' \right\} \psi \, dx \, d\mu, \quad m = 1, \dots, 5; \\ a^6(\psi, \phi) &= \int_{\Omega} \int_{-1}^1 \mu (\phi^- \partial_x \psi^+ - \psi^- \partial_x \phi^+) \, dx \, d\mu + \sum_{x \in \{0,1\}} \int_{-1}^1 |\mu| \phi^+(x, \mu) \psi^+(x, \mu) \, d\mu.\end{aligned}$$

Acknowledgment

This work was supported by the Excellence Initiative of the German federal and state governments and by the German Research Foundation through the Cluster of Excellence “Production technologies for high-wage countries”. Also, it was supported by the Grant GSC 111, the BMBF KinOpt Project, and by the DFG STE2063/1-1. We would also like to thank Eduard Bader and Mark Kärcher of RWTH Aachen for helpful discussions.

References

1. B. AHMEDOV, https://bitbucket.org/bahmedov/rom_optimalradiotherapy, (2015).
2. ———, *Approximation and Reduced Models for Optimal Radiotherapy*, PhD thesis, RWTH Aachen University, 2015 (in prep.).
3. I. BABUŠKA, *Error-bounds for finite element method*, Numer. Math., 16 (1970/1971), pp. 322–333.
4. I. BABUŠKA AND A. K. AZIZ, *Survey lectures on the mathematical foundations of the finite element method*, in The mathematical foundations of the finite element method with applications to partial differential equations (Proc. Sympos., Univ. Maryland, Baltimore, Md., 1972), Academic Press, New York, 1972, pp. 1–359. With the collaboration of G. Fix and R. B. Kellogg.
5. R. BECKER, H. KAPP, AND R. RANNACHER, *Adaptive finite element methods for optimal control of partial differential equations: Basic concept*, SIAM J. Control Optim., 39 (2000), pp. 113–132.

26 B. Ahmedov, M.A. Grepl, M. Herty

6. N. BELLOMO, N. K. LI, AND P. K. MAINI, *On the foundations of cancer modelling: selected topics, speculations, and perspectives*, Math. Models Methods Appl. Sci., 18 (2008), pp. 593–646.
7. N. BELLOMO AND P. K. MAINI, *Preface (special issue on cancer modelling)*, Math. Mod. Math. Appl. Sci., 15 (2005), pp. iii–viii.
8. ———, *Preface (special issue on cancer modelling)*, Math. Mod. Math. Appl. Sci., 16 (2006), pp. iii–vii.
9. ———, *Preface (special issue on cancer modelling)*, Math. Mod. Math. Appl. Sci., 17 (2007), pp. iii–vii.
10. C. BÖRGERS, *The radiation therapy planning problem*, vol. 110 of IMA Volumes in Mathematics and its applications, Springer-Verlag, 1999, pp. 1–16.
11. K. K. BUCCI, A. BEVAN, AND M. R. III, *Advances in radiation therapy: conventional to 3d, to IMRT, to 4d, and beyond*, CA Cancer J. Clin., 55 (2005), pp. 117–134.
12. W. DAHMEN, C. PLESKEN, AND G. WELPER, *Double greedy algorithms: Reduced basis methods for transport dominated problems*, ESAIM: Mathematical Modelling and Numerical Analysis, 48 (2014), pp. 623–663.
13. R. DAUTRAY AND J. L. LIONS, *Mathematical Analysis and Numerical Methods for Science and Technology (v.6)*, Springer, Paris, 1993.
14. H. EGGER AND M. SCHLOTTBOM, *Analysis and regularization of problems in diffuse optical tomography*, SIAM J. Math. Anal., 42 (2010), pp. 1934–1948.
15. ———, *A mixed variational framework for the radiative transfer equation*, Math. Models Methods Appl. Sci., 22 (2012), pp. 1150014, 30.
16. ———, *An L^p theory for stationary radiative transfer*, Appl. Anal., 93 (2014), pp. 1283–1296.
17. M. FRANK, M. HERTY, AND M. HINZE, *Instantaneous closed loop control of the radiative transfer equations with applications in radiotherapy*, ZAMM Z. Angew. Math. Mech., 92 (2012), pp. 8–24.
18. M. FRANK, M. HERTY, AND A. N. SANDJO, *Optimal radiotherapy treatment planning governed by kinetic equations*, Math. Models Methods Appl. Sci., 20 (2010), pp. 661–678.
19. M. FRANK, M. HERTY, AND M. SCHÄFER, *Optimal treatment planning in radiotherapy based on Boltzmann transport calculations*, Math. Models Methods Appl. Sci., 18 (2008), pp. 573–592.
20. A.-L. GERNER AND K. VEROY, *Certified reduced basis methods for parametrized saddle point problems*, SIAM J. Sci. Comput., 34 (2012), pp. A2812–A2836.
21. K. A. GIFFORD, J. L. H. JR., T. A. WAREING, G. FAILLA, AND F. MOURTADA, *Comparioson of a finite-element multigroup discrete-ordinates code with Monte Carlo for radiotherapy calculations*, Phys. Med. Biol., 51 (2006), pp. 2253–2265.
22. M. A. GREPL AND M. KÄRCHER, *Reduced basis a posteriori error bounds for parametrized linear-quadratic elliptic optimal control problems*, C. R. Math., 349 (2011), pp. 873–877.
23. H. HENSEL, R. IZA-TERAN, AND N. SIEDOW, *Deterministic model for dose calculation in photon radiotherapy*, Phys. Med. Biol., 51 (2006), pp. 675–693.
24. M. HERTY AND A. N. SANDJO, *On optimal treatment planning in radiotherapy governed by transport equations*, Math. Models Methods Appl. Sci., 21 (2011), pp. 345–359.
25. K. ITO AND K. KUNISCH, *Reduced order control based on approximate inertial manifolds*, Linear Algebra Appl., 415 (2006), pp. 531–541.
26. ———, *Reduced-order optimal control based on approximate inertial manifolds for non-linear dynamical systems*, SIAM J. Numer. Anal., 46 (2008), pp. 2867–2891.

27. M. KÄRCHER AND M. A. GREPL, *A certified reduced basis method for parametrized elliptic optimal control problems*, ESAIM Control Optim. Calc. Var., 20 (2014).
28. M. KÄRCHER, M. A. GREPL, AND K. VEROY, *Certified reduced basis methods for parametrized distributed optimal control problems*, SIAM J. Control Optim., (2015, submitted).
29. E. W. LARSEN, *Tutorial: The nature of transport calculations used in radiation oncology*, Transp. theory Stat. Phys., 26 (1997), p. 739.
30. R. J. LEVEQUE, *Python tools for reproducible research on hyperbolic problems*, Comput. Sci. Eng., 11 (2009), p. 19.
31. J. L. LIONS, *Optimal Control of Systems Governed by Partial Differential Equations*, Springer, 1971.
32. F. NEGRI, G. ROZZA, A. MANZONI, AND A. QUARTERONI, *Reduced basis method for parametrized elliptic optimal control problems*, SIAM J. Sci. Comput., 35 (2013), pp. A2316 – A2340.
33. A. T. PATERA AND E. M. RØNQUIST, *Reduced basis approximation and a posteriori error estimation for a Boltzmann model*, Computer Methods in Applied Mechanics and Engineering, 196 (2007), pp. 2925–2942.
34. G. ROZZA, D. B. P. HUYNH, AND A. T. PATERA, *Reduced basis approximation and a posteriori error estimation for affinely parametrized elliptic coercive partial differential equations*, Arch. Comput. Method. E., 15 (2008), pp. 229–275.
35. G. ROZZA AND K. VEROY, *On the stability of the reduced basis method for stokes equations in parametrized domains*, Comput. Methods Appl. Mech. Engrg., (2007), pp. 1244–1260.
36. D. M. SHEPARD, M. C. FERRIS, G. H. OLIVERA, AND T. R. MACKIE, *Optimizing the delivery of radiation therapy to cancer patients*, SIAM Rev., 41 (1999), pp. 721–744.
37. J. TERVO AND P. KOLMONEN, *Inverse radiotherapy treatment planning model applying boltzmann-transport equation*, Math. Models. Methods. Appl. Sci., 12 (2002), pp. 109–141.
38. J. TERVO, P. KOLMONEN, M. VAUHKONEN, L. M. HEIKKINEN, AND J. P. KAIPIO, *A finite-element model of electron transport in radiation therapy and related inverse problem*, Inv. Probl., 15 (1999), pp. 1345–1361.
39. J. TERVO, M. VAUHKONEN, AND E. BOMAN, *Optimal control model for radiation therapy inverse planning applying the Boltzmann transport equation*, Lin. Alg. Appl., 428 (2008), pp. 1230–1249.
40. F. TRÖLTSCH AND S. VOLKWEIN, *POD a - posteriori error estimates for linear-quadratic optimal control problems*, Comput. Optim. Appl., 44 (2009), pp. 83–115.
41. K. VEROY, C. PRUD'HOMME, D. V. ROVAS, AND A. T. PATERA, *A posteriori error bounds for reduced-basis approximation of parametrized noncoercive and nonlinear elliptic partial differential equations*, in Proceedings of the 16th AIAA Computational Fluid Dynamics Conference, 2003. AIAA Paper 2003-3847.